Thermoreversible, Epitaxial fcc ↔ bcc Transitions in Block Copolymer Solutions

Joona Bang, Timothy P. Lodge, and Xiaohui Wang
Departments of Chemistry and Chemical Engineering & Materials Science, University of Minnesota, Minneapolis, Minnesota 55455

Kristin L. Brinker and Wesley R. Burghardt
Department of Chemical Engineering, Northwestern University, Evanston, Illinois 60208
(Received 22 January 2002; published 31 October 2002)

Uncharged block copolymer micelles display thermoreversible transitions between close-packed and bcc lattices for a range of concentration, solvent selectivity, and copolymer composition. Using small-angle x-ray scattering on shear-oriented solutions, highly aligned fcc crystals are seen to transform epitaxially to bcc crystals, with fcc/bcc orientational relationships that are well established in martensitic transformations in metals. The transition is driven by decreasing solvent selectivity with increasing temperature, inducing solvent penetration of the micellar core.

DOI: 10.1103/PhysRevLett.89.215505 PACS numbers: 61.25.Hq, 61.50.Ks, 81.30.Hd, 83.80.Qr

Under appropriate conditions of temperature and concentration, spherical objects will pack onto a lattice. Neutral and charged colloids, surfactant and block copolymer micelles, star-branched and dendritic polymers, and atomic systems are all representative examples. In some cases, polymorphism is observed upon changing temperature, reflecting equilibrium order-order transitions (OOT) between two phases. The most prevalent of these is probably the transformation between close-packed [either face-centered cubic (fcc) or hexagonally close-packed (hcp)] and body-centered (bcc) symmetries, particularly in atomic systems [1,2]. Such a transition can herald a subtle change in the interaction potential; for example, it has been known for some time that potentials varying with interparticle separation as r^{-n} exhibit such a transition when $n \leq 6$ [3,4]. Similarly, charged colloids favor bcc lattices at low ionic strength, and fcc at high ionic strength, as the potential becomes steeper and more short ranged [5,6]. More recently, density functional theory and computer simulation have shown that star polymers can display fcc → bcc transitions either upon increasing the packing density or upon varying the number of branches [7,8]. It is therefore clear that delineation of fcc/bcc phase boundaries in well-characterized experimental systems can provide critical benchmarks for modern theory. Furthermore, it is also of interest to assess the degree of universality among the various systems exhibiting this particular transition.

Block copolymer micelles represent a particularly versatile class of materials for such studies, as the intermicellar potential may be readily tuned by solvent selectivity, chain architecture, and temperature even for the uncharged case. Here we report a detailed study of the thermoreversible fcc → bcc transition in block copolymer solutions. The transformation is shown for the first time to be epitaxial, through a pathway that echoes the response of simple metals. This result also confirms that the transition occurs at constant micelle number density. Furthermore, the underlying driving force involves solvent penetration of the micellar core, in contrast to previous cases where the properties of the corona were pivotal [9,10].

A polystyrene (PS)-polyisoprene (PI) diblock copolymer was synthesized by standard anionic polymerization procedures [11,12]. The resulting block molecular weights, $M_{PS} \approx 8000$ and $M_{PI} \approx 7000$ g/mol, were determined by a combination of size-exclusion chromatography and NMR. The polydispersity was 1.02. The PS-selective solvent diethyl phthalate was obtained from Aldrich, and purified according to standard procedures [11,12]. Solutions of 30 and 35 wt % were prepared gravimetrically. We have located identical thermoreversible fcc/bcc transitions for a variety of PS-PI diblocks, for a range of concentrations, and in several different solvents, and consequently these solutions are representative of a general phenomenon. Full phase diagrams (polymer volume fraction ϕ versus T) have been mapped out for several PS-PI in several solvents by a combination of small-angle x-ray scattering (SAXS), rheology, and static birefringence [11,12]. SAXS measurements taken for these solutions indicated fcc lattices at lower temperatures, bcc lattices at intermediate temperatures, and disordered solutions at high temperatures; for the solutions considered here, the fcc/bcc boundary was 35 °C. The reversibility of the OOT was established in each solution for which it was observed. In selected solutions, the position of the principal scattering peak q^* was monitored as a function of temperature, and $q^*(T)$ varied smoothly across the OOT, a necessary condition for epitaxy.

Two fundamental questions arise from these results: how does the transition happen, and why? In the case of atomic or colloidal systems, the transition must occur by spatial rearrangement of a conserved number of particles.

In the micellar case, however, one could envision a distinct change in the number of particles, for example, by micellar fusion, fission, dissolution, or simple expulsion of a few chains that reassemble in new, smaller micelles. However, as our results demonstrate, the transition is epitaxial, which is strong evidence that the number of particles is fixed during the transition. If the number of micelles were to change, the fixed ratio of fcc to bcc unit cells (i.e., 2) could not be readily satisfied.

The solutions were examined by SAXS in two *in situ* shear cells, to access two orthogonal axes. A Rheometrics DMTA parallel plate rheometer was modified to allow x rays to pass through the shear sandwich along the gradient direction (∇), and placed on the 6 m SAXS line at the University of Minnesota [13]. After shearing the sample for an hour at 30 °C (frequency 1 rad/s and strain amplitude 100%), a clear hexagonal pattern of reflections developed [Fig. 1(a)]. The susceptibility of fcc colloidal crystals and micellar solutions to shear ordering has been well documented; the predominant mode of alignment is the slippage of the densely packed {111} planes along the shear direction (**v**) with normals along ∇ [14–19]. The resulting SAXS pattern shows an inner set of six bright spots and a second set of six spots at larger q. After turning off the shear, the sample was heated to 40 °C (within the bcc region of the phase diagram). The 12 spots clearly remain, although significantly smeared azimuthally [Fig. 1(b)]. Furthermore, the inner six spots have moved outward (to larger q) and increased in intensity, and the outer spots have moved to smaller q. The same solutions were examined in a modified cone and plate shear cell [20] at the Advanced Photon Source, using similar shear and temperature histories, but with the x rays incident along the vorticity direction (**e**). As shown in Figs. 2(a) and 2(b), the number of observed reflections is greater, due to the increased flux and improved collimation, and the incident beam lies along a twofold rather than a threefold axis.

The epitaxial relationship for this transformation may be deduced after indexing the relevant reflections. It has previously been documented that shearing an fcc micellar solution generally produces a mixture of fcc ($ABCABC\ldots$) and hcp ($ABABAB\ldots$) packing of {111} planes along the gradient direction, and the same holds for the parallel plate rheometer [Fig. 1(a)] [15,16,18]. The inner six spots of the pattern arise from the {100} planes of hcp; a perfect fcc crystal with {111} planes normal to the beam would give no such reflections [17,19]. The outer spots, however, arise from a superposition of the {220} planes of the fcc stacking, with the flow direction aligned with the close-packed axis $[1\bar{1}0]$. Consequently, there are actually *two* epitaxial transformations (fcc → bcc and hcp → bcc), superimposed. The outer six "spots" of bcc in Fig. 1(b) arise from 200 reflections, indicating that the {220} planes of fcc transform into {200} planes of bcc.

Figure 2(a) provides a definitive assignment of an fcc crystal viewed along the [112] axis, with {111} planes oriented in the shear plane. (There are also four other spots which probably correspond to a small population of {111} planes oriented at $\pm 50°$ relative to the shear plane; these may be due to the inhomogeneity of the flow near the fluid surfaces. They have less than 1% of the intensity of the main reflections.) After heating into bcc in the absence of shear, the resulting pattern is indexed as a superposition of three distinct bcc crystals, viewed along the [211], [101], and $[1\bar{1}2]$ directions [Figs. 2(b) and 4(b)]. [A few weak additional reflections are also seen, which presumably originate from the "misaligned" fcc fraction in Fig. 2(a).] Interestingly, no clear evidence of any hcp stacking is evident; the way the different flow cells affect the fcc/hcp balance is beyond the scope of this Letter.

The proposed fcc → bcc mechanism is illustrated in Figs. 3(a) and 3(b). Figure 3(a) shows one distorted bcc unit cell embedded in two fcc unit cells, and one contraction axis and two expansion axes by which fcc can transform into bcc following the so-called Bain distortion [1]. There are three degenerate directions for contraction, leading ultimately to nine bcc unit cells; however, they are not degenerate with respect to the flow direction. The transformation is not a "pure" Bain distortion, in that the close-packed planes remain strictly parallel: $\{111\}_{fcc} \parallel \{110\}_{bcc}$ [2]. For each contraction axis there are three distinct orientations of the bcc unit cell in the close-packed (shear, **v**-**e**) plane, as illustrated in

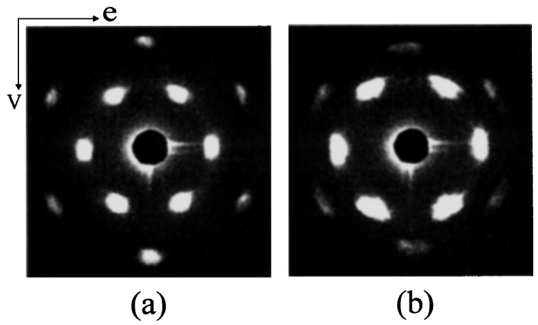

FIG. 1. SAXS patterns along the gradient direction (a) after shearing at 30 °C (fcc/hcp) and (b) after heating to 40 °C (bcc) without shear.

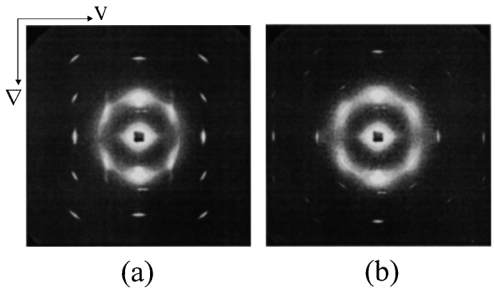

FIG. 2. SAXS patterns along the vorticity direction (a) after shearing at 30 °C (fcc) and (b) after heating to 40 °C (bcc) without shear.

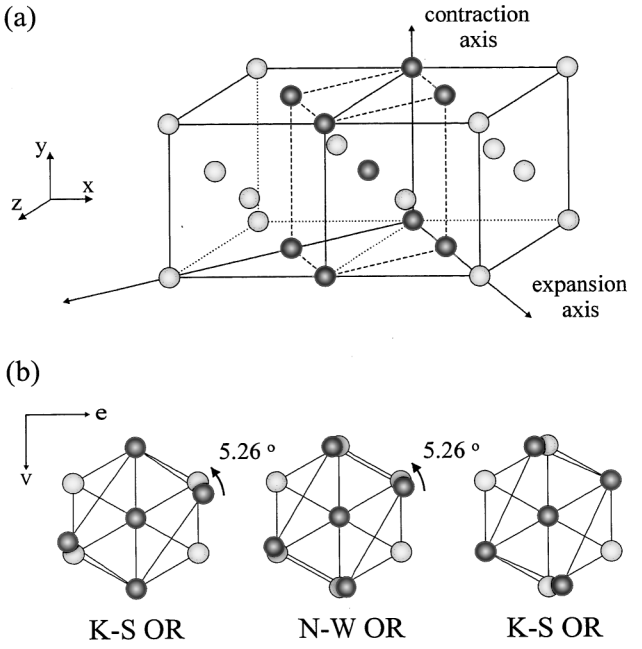

FIG. 3. (a) Distorted bcc unit cell embedded in two fcc unit cells and the Bain distortion axes for the transformation. (b) Superposition of close-packed {111} fcc (light spheres) and {110} bcc planes (dark spheres), illustrating the two Kurdjumov-Sachs and one Nishiyama-Wassermann orientation relationships.

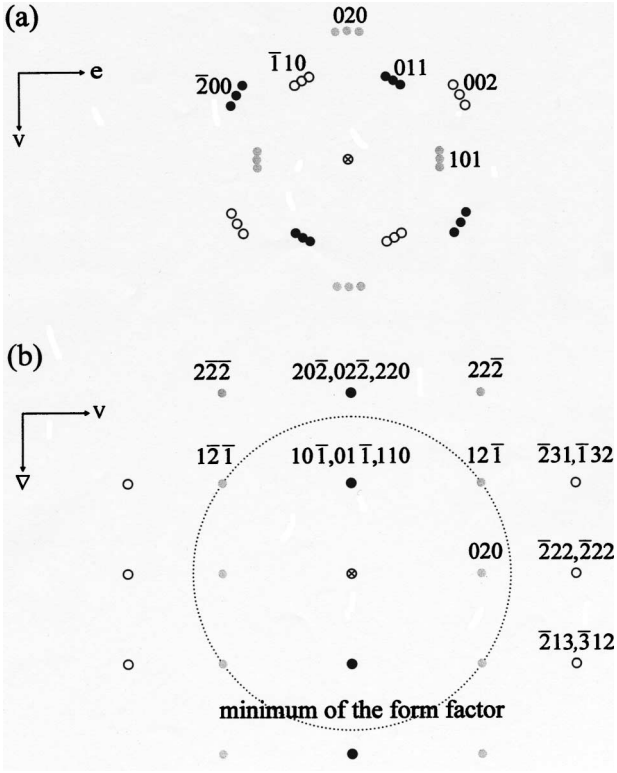

FIG. 4. Indexing bcc patterns (a) in the gradient and (b) vorticity directions. The diffraction patterns in (a) are from the $[01\bar{1}]$ (black circles), $[10\bar{1}]$ (gray circles), and [110] (white circles) beam directions. In (b) the open circles are the reflections in the [101] beam direction, with common reflections for the [211] and $[1\bar{1}2]$ beam directions shown in gray and in black for the [211], $[1\bar{1}2]$, and [101] beam directions.

Fig. 3(b). Two have close-packed directions that are coincident between fcc and bcc, which corresponds to the well-known Kurdjumov-Sachs (KS) orientational relationship (OR) in elemental crystals [2]. The third is obtained by a 5.26° in-plane rotation from either of the other two, leading to the Nishiyama-Wassermann (NW) OR [2]. In total, then, the nine bcc unit cells correspond to six KS and three NW ORs. Consequently, there are actually 18 002 and 18 011 reflections for the beam incident along ∇, collected in groups of three as shown in Fig. 4(a). The 5.26° rotations of the NW from the two KS ORs nicely account for the azimuthal smearing evident in Fig. 1(b). Furthermore, the increased intensity of the inner six spots is a direct consequence of the appearance of 110 reflections arising from the fcc → bcc transformation, whereas the inner six spots in Fig. 1(a) were only due to hcp stacking. The patterns in Figs. 2(b) and 4(b) are consistent with the superposition of three projections along a bcc crystal: the [101] x-ray beam direction (one of the three NW ORs) and the $[1\bar{1}2]$ and [211] directions (two of the six KS ORs). Thus, the beam incident along **e** shows reflections from only three of the nine bcc unit cells, except for the layer stacking (the 011, 022, etc. reflections). Note also that the form factor minimum diminishes the intensity of the 121 reflections.

This assignment of the transition epitaxy accounts for all the main features of the scattering along two different laboratory directions. The two observed ORs are consistent with the most prevalent observations of fcc/bcc grain boundaries in metals and simple alloys [1,2]. This mechanism has the appealing simplicity of preserving close-packed planes and (approximately) close-packed directions. In fact, rather than considering the transformation as a modified Bain distortion, it is probably more transparent to view it as occurring by relative slippage of the close-packed planes, followed by small in-plane strains. As described, for example, by Wentzcovitch and Krakauer [21], the fcc → bcc transformation involves relative motion of *A*, *B*, and *C* planes along the same $\langle 111\rangle_{\mathrm{fcc}}$ direction, whereas the hcp → bcc transformation involves *A* and *B* planes slipping in opposite directions. The hcp → bcc transformation results in the same nine distinct bcc unit cells as does fcc → bcc; the analogous ORs to KS and NW are known as the Burgers and Pitsche-Schrader ORs, respectively [2].

We now turn to the second question posed above, namely, what drives the transition? The first point to note is that the corona block, PS, is under good solvent conditions over the relevant temperature range, so we may exclude changes in corona conformation as an important factor. This differs from poly(ethyleneoxide-*b*-butylene oxide) (EB) diblocks in water, which undergo a thermoreversible bcc → fcc transition upon heating [9]. This transformation was attributed to a significant contraction of the E corona as the solvent quality decreased

with increasing temperature, thereby inducing a "hairy" to "crewcut" transition in the micelles. We propose that the crucial feature in our case is the decreasing selectivity of the solvent with increasing temperature. Consequently, the solvent begins to penetrate the isoprene-rich micellar core, thereby increasing the overall micellar radius. The close-packed micelles respond to this increased repulsion by rearranging to the looser bcc lattice. In short, the transition is driven by core swelling. Three additional pieces of evidence may be cited for this interpretation. First, dynamic light scattering measurements of similar polymer/solvent combinations at lower concentrations ($\phi \approx 0.01$) indicate that the hydrodynamic radius of the micelles increases slightly with increasing temperature over the temperature range where the fcc/bcc transition is found [12]. Second, in some solutions a disordered suspension of micelles at low temperature undergoes a "reentrant" ordering transition to fcc upon heating, suggesting that the effective radius of the micelles has increased [11,12]. Third, density functional theory and computer simulations for highly branched star polymers indicate that, under appropriate conditions, an fcc $\rightarrow$ bcc transition can be induced by increasing the packing fraction (i.e., the micellar radius increases) [7,8].

An alternate hypothesis should also be considered, namely, that as the solvent selectivity diminishes, the mean aggregation number of the micelles decreases at constant micellar radius. As the solvent enters the core, the interfacial tension at the core/corona interface goes down, and a smaller number of copolymers per unit area are required. This scenario is also supported by the aforementioned calculations, in that the fcc $\rightarrow$ bcc transition can be induced by reducing the number of star arms [7,8]. In addition, the principal spacing of the cubic lattices, $2\pi/q^*$, decreases steadily across the transition, suggesting an overall increase in the number of micelles with temperature. However, as noted above, the epitaxy of the transition argues against an abrupt change in the number of micelles at the transition. In summary, then, the transition is driven by the change in solvent selectivity via some combination of micellar swelling and a decrease in the aggregation number with increasing temperature, with the former factor likely predominant.

It would be instructive to apply the successful self-consistent mean-field theory to this problem, as it is potentially capable of resolving this level of "fine structure" in the behavior of block copolymer mesophases [22]. From a broader perspective, the window of bcc that intervenes between fcc and disordered liquid in many of these block copolymer solutions is reminiscent of the behavior of atomic systems, in fact, for a significant fraction of the periodic table. In this sense, these results support the conjecture that a bcc phase is generally thermodynamically preferred near the melting line, for weakly first-order melting transitions, for universal entropic considerations [23].

This work was supported by the National Science Foundation, through the University of Minnesota MRSEC (DMR-9809364), through DMR-9901087 (T. P. L.), and through the Northwestern University MRSEC (DMR-0076097). Use of the Advanced Photon Source was supported by the U.S. Department of Energy, Basic Energy Sciences, Office of Science, under Contract No. W-31-109-Eng-38. Experiments were conducted at DND-CAT, which is supported by DuPont, Dow, NSF (DMR-9304725), the Illinois Department of Commerce, and Grant No. IBHE HECA NWU 96.

[1] K. Shimizu and Z. Nishiyama, Metall. Trans. **3**, 1055–1068 (1972); Z. Nishiyama, *Martensitic Transformation* (Academic Press, New York, 1978).
[2] U. Dahmen, Acta Metall. **30**, 63–73 (1982).
[3] W. G. Hoover, D. A. Young, and R. Grover, J. Chem. Phys. **56**, 2207–2210 (1972).
[4] B. B. Laird and A. Haymet, Mol. Phys. **75**, 71 (1992).
[5] Y. Mounovoukas and A. P. Gast, J. Colloid Interface Sci. **128**, 533 (1988).
[6] M. O. Robbins, K. Kremer, and G. S. Grest, J. Chem. Phys. **88**, 3286 (1988).
[7] M. Watzlawek, C. N. Likos, and H. Lowen, Phys. Rev. Lett. **82**, 5289–5292 (1999).
[8] B. Groh and M. Schmidt, J. Chem. Phys. **114**, 5450–5456 (2001).
[9] I. W. Hamley, J. A. Pople, and O. Diat, Colloid Polym. Sci. **276**, 446 (1998).
[10] G. A. McConnell and A. P. Gast, Macromolecules **30**, 435 (1997).
[11] K. J. Hanley, T. P. Lodge, and C.-I. Huang, Macromolecules **33**, 5918–5931 (2000).
[12] T. P. Lodge, B. Pudil, and K. J. Hanley, Macromolecules **35**, 4707–4717 (2002).
[13] C.-Y. Wang and T. P. Lodge, Macromolecules **35**, 6997 (2002).
[14] B. J. Ackerson and N. A. Clark, Phys. Rev. A **30**, 906 (1984).
[15] W. Loose and B. J. Ackerson, J. Chem. Phys. **101**, 7211 (1994).
[16] G. A. McConnell, M. Y. Lin, and A. P. Gast, Macromolecules **28**, 6754–6764 (1995).
[17] O. Diat, G. Porte, and J.-F. Berret, Phys. Rev. B **54**, 14 869–14 872 (1996).
[18] I. W. Hamley *et al.*, J. Chem. Phys. **108**, 6929–6936 (1998).
[19] F. R. Molino *et al.*, Eur. Phys. J. B **3**, 59–72 (1998).
[20] F. E. Caputo and W. R. Burghardt, Macromolecules **34**, 6684 (2001).
[21] R. M. Wentzcovitch and H. Krakauer, Phys. Rev. B **42**, 4563 (1990).
[22] M. W. Matsen and F. S. Bates, Macromolecules **29**, 1091–1098 (1996).
[23] S. Alexander and J. McTague, Phys. Rev. Lett. **41**, 702–705 (1978).